Spotlighting Recent Advances in Liquid-Crystal Devices for Beam-Steering Applications

With their continuous tunability, wide field of view, and high efficiency, liquid crystal devices are strong candidates for beam-steering applications. Here, we summarize some recent advances in liquid crystal beam-steering devices.

by **Kun Yin, Ziqian He, and Shin-Tson Wu**

PRECISELY POSITIONING AND STEERING A LASER BEAM OR light ray has enabled widespread applications, including light detection and ranging (LiDAR) for self-driving vehicles,[1,2] high-resolution head-mounted displays (HMDs),[3] eye tracking for fovea displays,[4] folding the optical path in augmented reality (AR) displays,[5] microscopy,[6] and laser micromachining.[7] Along the way, various beam-steering methods have been developed. Generally, they can be divided into two groups: mechanical and nonmechanical beam controls. Mechanical approaches include scanning/rotating mirrors,[8] rotating prisms,[9] and micro-electro-mechanical-system (MEMS) mirrors.[10] Nonmechanical options include acousto-optic deflectors,[11] electrowetting,[12] and liquid crystal (LC) technologies.[13]

Traditional mechanical beam-steering devices often are heavy and bulky with relatively large power consumption. In contrast, recently developed mechanical and nonmechanical beam steerers strive to overcome these shortcomings. LC-based beam steerers are strong contenders in this arena, as they can be lightweight and compact, with low power and cost.

With this potential in mind, here we consider the physical principles of existing LC-based beam steering devices. Next, we dive into different types of LC-based beam steerers before finally summarizing their pros and cons.

Classifying the Operation Principles of LC-Based Beam Steering

The operation principles of LC-based beam steerers are classified into three categories. The first type is blazed grating, which belongs to thin grating or one-dimensional grating (the Raman-Nath regime). The diffraction angles are described by the following grating equation:

$$n_{(1,2)}\sin\theta_{m(1,2)} = n_1\sin\theta_{in} - m\frac{\lambda_0}{\Lambda} \qquad (1)$$

where $n_{(1,2)}$ is the refractive index in medium 1 (or 2), $\theta_{m,(1,2)}$ is the angle of mth diffraction order in medium 1 (or 2), θ_{in} is the incident angle, Λ is the grating period, and λ_0 is the wavelength in vacuum. **Fig. 1a** depicts the thin grating's schematic diagram.

The second category is volume grating. Unlike thin grating, volume grating belongs to thick gratings (the Bragg regime). The Bragg condition can be described as

$$2d\sin\theta = m\lambda \qquad (2)$$

where d is the period, θ is the angle between the incident beam and the Bragg plane, and λ is the wavelength in the medium. **Fig. 1b** depicts a 1D Bragg grating. A distinct feature of these gratings
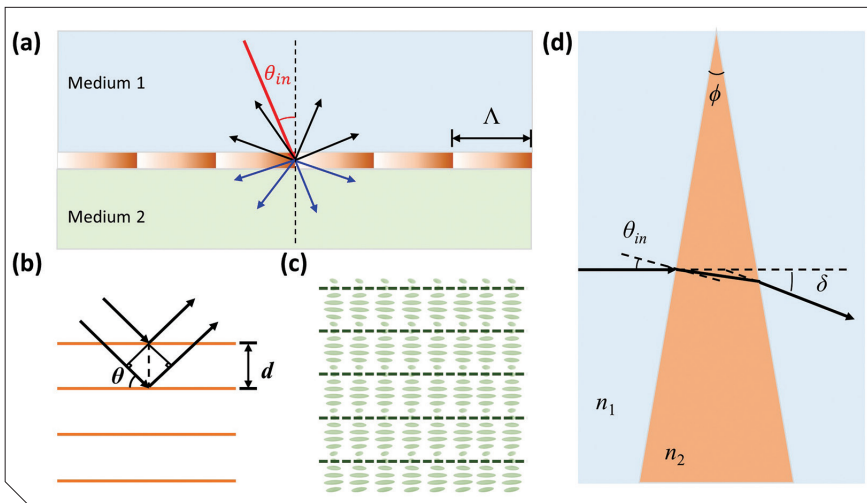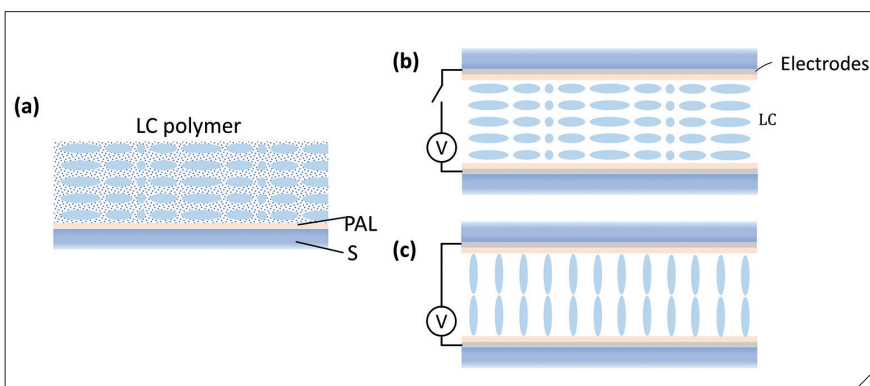
Fig. 1.

(a) Schematic plot of a grating in Raman-Nath regime. Multiple diffraction orders in both forward (blue arrows) and backward (black arrows) coexist. (b) Schematic plot of Bragg reflection in a periodic structure, and (c) a liquid crystal (LC) Bragg grating based on helical cholesteric structure. (d) Schematic diagram of a prism-based beam deflector.

is the high sensitivity of incident wavelengths and angles. A well-known example of the LC-based Bragg structure is cholesteric liquid crystal (CLC), as **Fig. 1c** shows.

We can form a CLC structure by doping some chiral compounds into a rod-like nematic host. In the CLC phase, LC directors rotate continuously along the stacking direction, and a helical structure exists perpendicular to the layer planes (dark green dashed lines). Establishing a Bragg reflection usually requires ~10 pitches. The reflection also greatly depends on the incident angle and wavelength. By dynamically tuning the pitch length, the angle and wavelength dependency change accordingly. This is the principle employed for volume-grating beam steering. Through changing

Fig. 2.

Schematic illustration of the structure of (a) a passive Pancharat-nam-Berry deflector (PBD) made of a liquid crystal polymer and an active PBD made of liquid crystal at (b) voltage-on and (c) voltage-off state.[15] (PAL: photo-alignment layer; S: substrate; V: voltage.)

the period, within the bandwidth, the diffraction angle for a given wavelength varies. Another distinct feature is that the thick grating can steer an incident light to a large angle with high efficiency while the thin grating hardly can achieve that.

The third mechanism is prism-type beam steering. This differs from the previous two, in that it's based on refraction rather than diffraction. As **Fig. 1d** shows, when a light beam passes through a prism, refraction upon both sides of the prism leads to a deviation of incident light. When the prism angle and incident angle are small, the prime angle can be approximated as

$$\delta \approx \left(\frac{n_2}{n_1} - 1\right)\Phi \qquad (3)$$

In **Eq. (3)**, ϕ denotes the prism angle, n_1 the refractive index of background medium, and n_2 the prism refractive index. For such a thin prism, the angular deviation is insensitive to the angle of incidence (θ_{in}). Based on this principle, we tune the deviation angle by changing a refractive index.

Here, we should be clear that research on LC-based beam-steering devices is ongoing. Apart from the aforementioned work, new methods are emerging—for example, micromirrors with LC elastomer fibers and tuning the LC microlens' curvature. These methods are under active development and are not ready for practical applications, but they may find interesting applications in the future.

Configuring LC Beam-Steering Devices

Next, we focus on three device configurations: Pancharat-nam-Berry phase grating, Bragg volume grating, and LC *cladding* (a coating or covering on the material's structure) waveguide. These configurations correspond to the three different operating principles (Raman-Nath, Bragg, and prism-type beam steering, respectively).

HARNESSING PANCHARATNAM-BERRY PHASE DEFLECTORS
With intrinsic polarization sensitivity and high diffraction efficiency, the Pancharatnam-Berry deflectors (PBDs)[14] made of liquid crystals or LC polymers are promising candidates for nonmechanical beam steering. As a special case of PB optical elements, the PBDs can be established by patterning half-wave plates with an in-plane linearly rotating optical axis, as **Fig. 2a** depicts. Their working mechanism can be explained by the Jones matrix:

$$R(-\varphi)W(\pi)(\varphi)J_\pm = -je^{\pm 2j\varphi}J \qquad (4)$$

where R is the rotation matrix, ϕ the optical axis orientation angle, W(π) is the half-wave retardation matrix, and J± is the

Jones vector of right-handed circularly polarized (RCP) or left-handed circularly polarized (LCP) input light. With a linearly rotating optical axis, the PBD can deflect a circularly polarized normal incident light into first order with ~100 percent diffraction efficiency in theory and flip the light's handedness.

Usually PBDs are fabricated through a polarization holography and photo-alignment method, transferring the linearly rotating polarization pattern to LC directors' orientation. According to the driving method, PBDs can be categorized into two types: passive and active. Passive PBDs are generally prepared by coating a reactive mesogen layer on an aligned surface, as **Fig. 2a** shows. The active PBDs are fabricated by filling LC into a patterned cell with transparent electrodes and a photo-alignment layer, as **Figs. 2b** and **2c** show. If the applied voltage is high enough, the LC directors will be reoriented along the electric field directions so that the deflection effect of PBD vanishes.

For a passive PBD, the deflecting angle can be switched by controlling the input polarization state, as depicted in **Fig. 3a**. For an active PBD, the input beam can be switched between 0th and ±1 diffraction orders, simply by applying a voltage to the PBD, as illustrated in **Fig. 3b**. Based on the polarization selectivity, we can use either a passive or active PBD to steer a laser beam. In this scheme, a half-wave plate as the polarization rotator—such as a 90° twisted-nematic LC cell—is placed in front of the PBD to dynamically select the input polarization.

Fig. 3c depicts a passive PBD beam steering stage, which contains two passive PBDs and two switchable half-wave plates. When both waveplates are in the same state (that is, both ON or both OFF), the diffraction from the first PBD is compensated by the second one. But when these two waveplates are in the opposite states, the incident beam can be diffracted into the positive or negative order. As a result, we obtain three steering directions. In **Fig. 3d**, using an active PBD and a switchable half-wave plate also can steer the incident light to three different directions.

WORKING WITH BRAGG VOLUME GRATINGS
LC-based Bragg volume gratings own the ability to split and diffract the beam into different directions. Through careful design, volume gratings have several distinctive features: strong polarization selectivity, high diffraction efficiency, and large deflection angles.

Polarization volume grating (PVG) is a recently developed LC-based volume grating.[16] **Fig. 4a** illustrates the LC director distribution of a reflective PVG. The Bragg period and periods along the
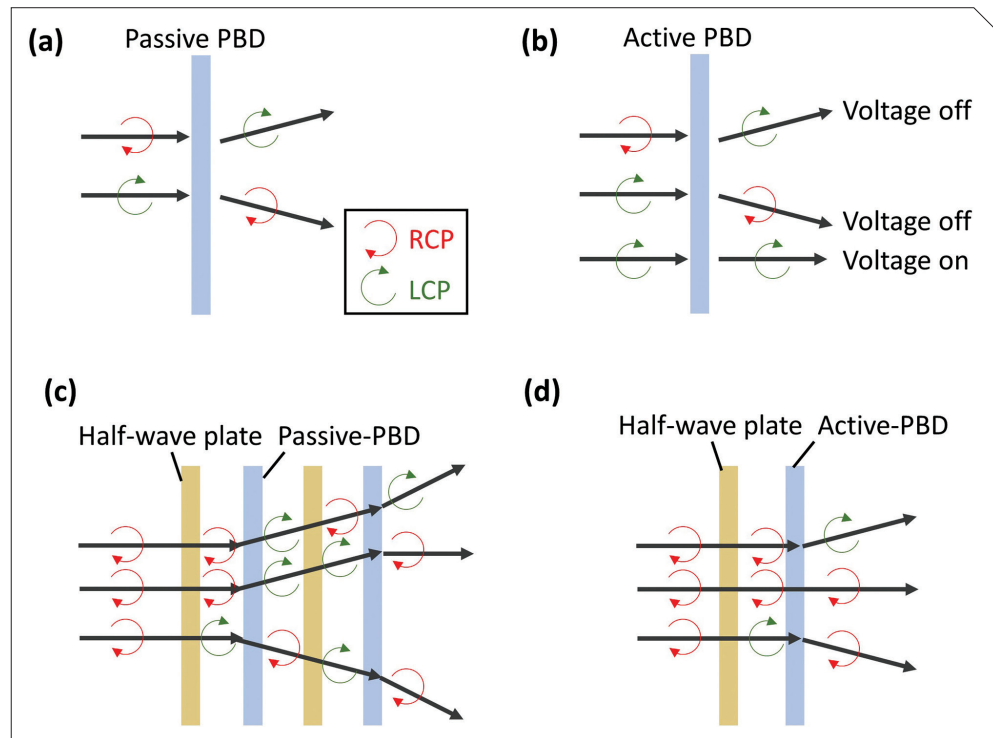

Fig. 3.

Schematic illustration of the beam-steering approaches using PBD: (a) a passive PBD, (b) an active PBD, (c) two passive PBDs with two polarization rotators, and (d) ab active PBD with a polarization rotator.
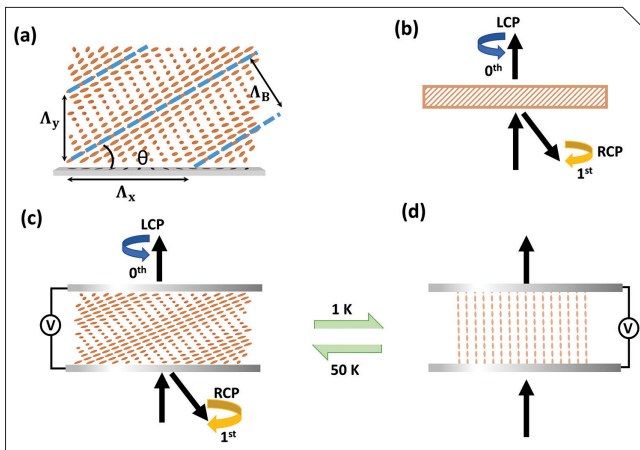
x and y directions are Λ_B, Λx, and Λy, respectively. This asymmetrically self-organized structure enables unique polarization selectivity, where only the light with the same chirality as the helical twist will be diffracted.

Fig. 4b depicts the diffracted and transmitted beams' polarization states for a typical reflective PVG. Here, we assume the PVG is right-handed along the incident direction. Therefore, such a PVG can diffract the RCP light to the first order and keep its polarization state. Meanwhile, the LCP light will pass through the PVG without changing its polarization state. Besides, a PVG possesses stronger selectivity in wavelength and angle than a thin grating and this should be considered when targeting on a specific wavelength. The working central wavelength can be designed precisely by the modified Bragg condition:

$$\lambda_B = 2n\Lambda_B\cos\theta \qquad (5)$$

where n is the average refractive index of the employed LC material, and θ is the slant angle defined as $\tan\theta = \Lambda_y/\Lambda_x$. Typically, the bandwidth ranges from 30 to 50 nm, which is related to the birefringence of the employed LC material. The field of view (angular response) for the central wavelength is around 20°.

Compared to PBDs, PVGs possess a larger diffraction angle. With proper organization, the diffraction angle can reach 70° or even larger, while keeping diffraction efficiency more than 90 percent of a single PVG. These unique advantages make PVG

a promising candidate for beam-steering applications. While PVGs can be applied as a passive beam steerer with the help of a fast-switching polarization rotator, active PVGs also can be achieved by assembling a cell with a dual-frequency LC material. As **Figs. 4c** and **4d** show, after applying a voltage of 50 V (1 kHz), the LC directors are reoriented to the homeotropic state where the Bragg grating effect disappears. Switching the frequency of the applied voltage to 50 kHz can turn it back to the Bragg grating state.

INCREASING INTERACTION LENGTHS VIA THE LC CLADDING WAVEGUIDE

As **Equation (3)** mentions, LC prisms can achieve only a relatively small steering angle because of the limitation in the LC refractive index change and prism geometry. However, the interaction length can be increased dramatically by guiding light in a waveguide, as Vescent Photonics demonstrated roughly a decade ago.[17] This special waveguide consists of LC cladding, a Si_3N_4 core, and glass cladding. The beam steering can be controlled simply by manipulating the evanescent wave in the LC cladding region. By applying voltage on the LC, we obtain different refractive index contrasts between the waveguide core and cladding. Depending on the applied voltage, the different refractive index contrasts result in different light directions. With the electrodes' special design, a remarkably large steering angle (up to 270°) has been demonstrated.

Here, we propose a beam-steerer concept that combines an LC-cladding waveguide with resistive electrodes. **Fig. 5** shows the configuration. In fact, the structure is similar to the Vescent Photonics device, except that the top electrodes are replaced by resistive electrodes. Through creating a refractive index gradient and interacting with evanescent waves, the LC thickness can be thin, and the accumulated phase gradient can be large, meaning that large-angle beam steering with fast response time is achievable. Ideally, a single resistive electrode **(Fig. 5a)** can provide continuous beam steering because it is refractive. However, the dimension is so limited (~150 μm wide) that it only works for small-sized beams. To enlarge the aperture size, an array of resistive electrodes is needed **(Fig. 5b)**.
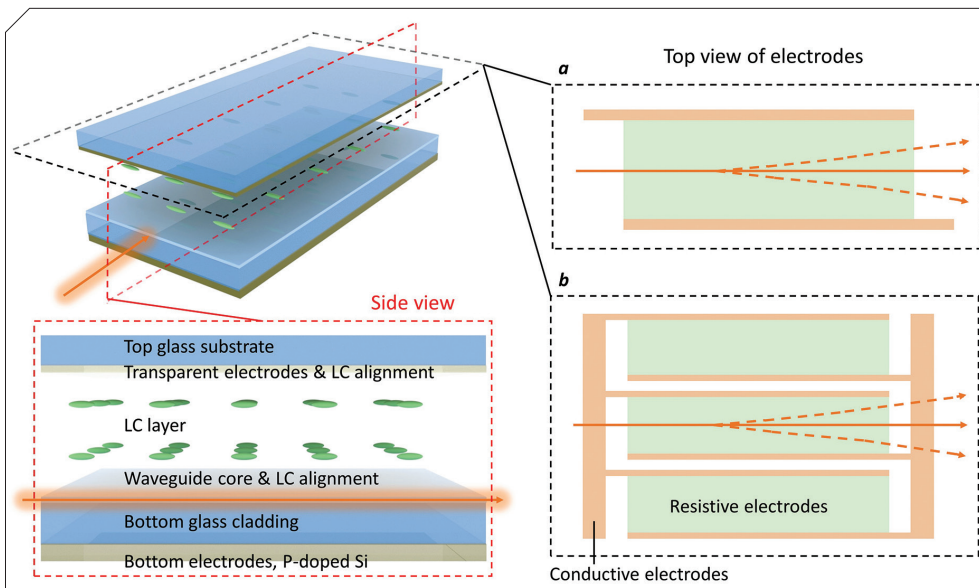
Application Example

Next, to illustrate this technology's applicability, we consider an example that stems from the upswing of interest in nonmechanical beam steering based on patterned LCs. In a LiDAR system, the beam is directed to a receiver to track precisely and with good stability, and LiDAR needs to steer the beams over the desired field of view and precision. Thus here, we take the patterned LC-based PBD as an example to discuss its performances in a target LiDAR system.

DIFFRACTION EFFICIENCY
PBD's single efficiency can reach more than 90 percent

over a wide spectral range (for example, 400–700 nm), and it can be close to 100 percent at a specific wavelength. In addition, as long as the LC thickness meets the half-wave condition, the most efficient operating wavelength can be designed from the visible to near-infrared spectral range.[14]

FIELD OF VIEW

The field of view is directly related to the diffraction angle. Generally, the incident angle can be ±10° while maintaining a high efficiency. For a passive PBD, if we apply a multilayer structure, the field of view can be increased dramatically to ±30° or even larger with a designed wavelength and diffraction angle.[5,14]

RESPONSE TIME

For an active PBD, the response time can be controlled by fine-tuning the viscosity of employed LC material and the cell gap. For an active PBD (working wavelength $\lambda = 633$ nm), the switching time between the zeroth order and first order is less than 1 millisecond (ms).[14]

STEERING ANGLE

The steering range of PBD-based LiDAR can be increased by cascading passive and active PBDs together. **Fig. 3** illustrates the working principles. The resolution is determined by each PBD's diffraction angle (it can narrow down to 1° or smaller, depending on the requirement).

DEVICE SIZE

One of the biggest advantages of PBD is its large working area. Through the interference fabrication process, PBD's clear aperture size can be larger than 2 inches, depending on the exposure beam size.[5,14]

Overall, these performance capabilities should make this approach an interesting option for beam-steering requirements in applications such as LiDAR.

Here, we briefly reviewed the recent advances of three different LC beam steerers and discussed their operation principles and applications. Today, traditional mechanical beam-steering devices are reasonably robust. Yet technical issues remain—including their relatively short lifetime and substantial weight, power consumption, and cost. We expect that eventually, LC-based beam steerers with lightweight, compact size, low power, and low cost will find widespread applications in novel optical systems. ⬛

References

[1] Collis RTH. LiDAR. Applied Optics. 1970;9(8):1782-1788.

[2] Lumotive. High-performance, solid-state LIDAR powered by liquid crystal metasurface technology [Internet]. 2020. Available from: https://www.lumotive.com/.

[3] Zhan T et al. Augmented reality and virtual reality: perspectives and challenges. iScience. 2020;23(8):101397.

[4] Tan G et al. Foveated imaging for near-eye displays. Optics Express. 2018;26(19):25076-25085.

[5] Yin K, Lin HY, and Wu ST. Chirped polarization volume grating for wide FOV and high efficiency waveguide-based AR displays. J. Society for Information Display (JSID). 2020;28:368-374.

[6] Betzig E and Trautman JK. Near-field optics: microscopy, spectroscopy, and surface modification beyond the diffraction limit. Science. 1992;257:189-195.

[7] Gattass RR and Mazur E. Femtosecond laser micromachining in transparent materials. Nature Photonics. 2008;2:219-225.

[8] Wehr A and Lohr U. Airborne laser scanning—an introduction and overview. ISPRS J. Photogrammetry and Remote Sens. 1999;54(2-3):68-82.

[9] Duncan BD, Philip JB, and Vassili S. Wide-angle achromatic prism beam steering for infrared countermeasure applications. Optical Engineering. 2003;42(4):1038-1047.

[10] Hofmann U, Janes J, and Quenzer HJ. High-Q MEMS resonators for laser beam scanning displays. Micromachines. 2012;3(2):509-528.

[11] Meyer RA. Optical beam steering using a multichannel lithium tantalite crystal. Applied Optics. 1972;11(3):613-616.

[12] Cheng J and Chen CL. Adaptive beam tracking and steering via electrowetting-controlled liquid prism. Applied Physical Letters. 2011;99(19):191108.

[13] Resler DP et al. High-efficiency liquid-crystal optical phased-array beam steering. Optics Letters. 1996;21(9):689-691.

[14] Zhan T et al. Pancharatnam-Berry optical elements for head-up and near-eye displays. J. Optical Society of America B. 2019;36 (5):D52-D65.

[15] He Z et al. Liquid crystal beam steering devices: principles, recent advances, and future developments. Crystals. 2019;9(6):292. Available from: https://doi.org/10.3390/cryst9060292.

[16] Yin K et al. Polarization volume gratings for near-eye displays and novel photonic devices. Crystals. 2020:10(7);561. Available from: https://doi.org/10.3390/cryst10070561.

[17] Davis SR et al. Liquid crystal waveguides: new devices enabled by > 1000 waves of optical phase control. Proc. International Society for Optical Engineering (SPIE). 2010 Feb. 12; San Francisco, CA. 76180E. Available from: https://doi.org/10.1117/12.851788.

Kun Yin is working toward a Ph.D. from CREOL, the College of Optics and Photonics, University of Central Florida, Orlando. Her current research interests include novel optical components based on liquid crystal materials and optical system design for augmented reality and virtual reality displays. She can be reached at *kunyin@knights.ucf.edu*.

Ziqian He is working toward a Ph.D. at CREOL, the College of Optics and Photonics, University of Central Florida. His research focuses on perovskite nanomaterials, liquid crystal devices, and displays. He can be reached at *zhe@knights.ucf.edu*.

Shin-Tson Wu is a Pegasus professor at CREOL, the College of Optics and Photonics, University of Central Florida. He is among the first six inductees of the Florida Inventors Hall of Fame (2014), a Charter Fellow of the National Academy of Inventors (2012), and a Fellow of SID, IEEE, the Optical Society (OSA), and the International Society for Optics and Photonics (SPIE). He can be reached at *swu@creol.ucf.edu*.